

Sericin ameliorated dysmorphic mitochondria in high-cholesterol diet/streptozotocin rat by antioxidative property

Sumate Ampawong¹, Duangnate Isarangkul² and Pornanong Aramwit³

¹Department of Tropical Pathology, Faculty of Tropical Medicine, Mahidol University, Bangkok 10400, Thailand; ²Department of Microbiology, Faculty of Science, Mahidol University, Bangkok 10400, Thailand; ³Bioactive Resources for Innovative Clinical Applications Research Unit and Department of Pharmacy Practice, Faculty of Pharmaceutical Sciences, Chulalongkorn University, Bangkok 10330, Thailand

Corresponding author: Pornanong Aramwit. Email: aramwit@gmail.com

Impact statement

The present work provides new insights regarding the antioxidative effect of sericin in (i) reducing blood cholesterol, (ii) improving liver and heart mitochondrial structures, (iii) maintaining endoplasmic reticulum integrity in exocrine pancreatic glands, and (iv) inhibiting fat deposition in the liver. Electron microscopic, histopathologic, immunohistochemical, and biochemical studies were performed. All of the results demonstrate the efficacy of sericin as a candidate for development of a functional food or adjunctive therapeutic agent against non-communicable diseases such as hypercholesterolemia.

Abstract

Sericin has been implicated in lower cholesterolemic effect due to its properties with several mechanisms. Mitochondria are one of the most important targets to be affected in high blood cholesterol and glucose conditions. The protective role of sericin on mitochondria remains doubtful. To examine this role, electron microscopic, histopathologic, immunohistochemical, and biochemical studies were performed in a high-cholesterol diet/streptozotocin rat model. The results demonstrated that sericin reduced blood cholesterol without hypoglycemic effect. Sericin alleviated dysmorphic mitochondria in heart and liver but not in kidney and also decreased peculiar endoplasmic reticulum in the exocrine pancreas. In addition, sericin decreased hepatic steatosis and preserved zymogen granule referable to the decline of reactive oxygen species production in hepatic mitochondrial extraction and down-regulation of malondialdehyde expression in the liver and exocrine pancreas however

irrelevant to lipase activity. This study suggests that sericin has antioxidative property to reduce blood cholesterol by means of diminishing fat deposit in hepatocyte and improves mitochondria and endoplasmic reticulum integrities.

Keywords: Cholesterol, diabetes mellitus, endoplasmic reticulum, mitochondria, oxidative stress, sericin

Experimental Biology and Medicine 2017; 242: 411–421. DOI: 10.1177/1535370216681553

Introduction

Mitochondria are known as the cell's powerhouse because they generate energy as adenosine triphosphate during electron transport and the respiratory chain reaction.¹ Living cells cannot function and survive without mitochondria. It is well described that mitochondrial defect and oxidative stress implicate to several kinds of diseases such as non-alcoholic fatty liver,^{2,3} diabetic cardiac diseases,⁴ diabetic kidney diseases,⁵ hypercholesterolemia,⁶ hypertension,⁷ and neurodegenerative diseases.⁸ To develop new candidates for adjunctive therapy, many studies have been suggested that some natural products can alleviate those kinds of mentioned diseases due to their antioxidative property and probably lead to promote mitochondrial activities.^{9–11} Sericin, water-soluble silk cocoon protein, is thought to reduce the effects of hypocholesterolemia through antioxidative effects,¹² the inhibition of hepatic lipogenesis,¹³ and reduced cholesterol absorption from the intestine.¹⁴

Moreover, sericin also alleviates blood glucose tolerance in patients with high cholesterol.¹³ However, it remains unclear whether sericin can improve mitochondrial integrity and function simultaneously to lower blood cholesterol and glucose with antioxidant effects.

In this study, we conducted an *in vivo* model, hypercholesterolemic and hyperglycemic rat induced by high-cholesterol diet and streptozotocin (STZ) injection, to demonstrate the protective effect of sericin to mitochondria in affected organs due to its antioxidative property. Clinical blood chemistry was measured for lipid and carbohydrate profiles. Electron microscopic studies were performed to characterize dysmorphic mitochondria from heart, liver, and kidney extractions. Mitochondrial ultrastructural changes in heart, liver, kidney, and pancreas were also compared. Immunohistochemical studies were used to identify oxidative (malondialdehyde [MDA]) and antioxidative (super-oxide dismutase [SOD]) markers in mentioned

tissues. Finally, reactive oxygen species (ROS) production was biochemically measured in hepatic mitochondrial extraction. To our knowledge, this is the first study that provides insight regarding the effect of silk sericin on high cholesterol/STZ-induced mitochondrial dysfunction and proposes guidelines for therapeutic use.

Materials and methods

Silkworm cocoons and sericin extraction

In the present study, silkworm cocoons, *Bombyx mori*, were provided by Chul Thai Silk Co., Ltd, Phetchabun province, Thailand. There are several methods for sericin extraction such as heat, acid, alkali, and urea treatments that result in difference of physical and biological properties.^{15,16} Since heat-extracted sericin is considered as pure sericin without any chemical contamination and our previous study demonstrated that this type of sericin provides appropriate biological activities and safe, it was used in this experiment. Amino acid composition in heat-extracted sericin is presented in Table 1.¹⁶ For sericin extraction, fresh cocoon shells were cut into pieces and autoclaved in purified water at 120°C for 60 min. The supernatant was collected, filtered, frozen, and then lyophilized.

Ethics statement

The animal study was approved by the Faculty of Medicine, Chulalongkorn University Animal Care and Use Committee, Bangkok, Thailand (Approval No. 16/2558). Fifteen healthy female Wistar rats (eight weeks old, 200–300 g) were obtained from the National Laboratory Animal Center, Mahidol University. They were quarantined and acclimatized for seven days after receiving and housed under strict hygienic conventional conditions of a 12 h dark/light cycle with temperature and humidity control.

Induction hypercholesterolemic and hyperglycemic rats

Rats were randomly allocated in three groups (five of each): normal diet without induction (sham) and the high-cholesterol diet/STZ (C/STZ)-induced rats with or without sericin at a dosage of 1000 mg/kg/day, as described by Limpeanchob *et al.*¹⁴ Sham rats were fed *ad libitum* with standard diet from Perfect Companion Ltd, Thailand (nutritional ingredients: 24.5% total protein, 2.24% fat, 3.34% fiber, 5.23% ash, 0.456% sodium chloride, 0.123% calcium, and 0.965% phosphorus). In this formula, legumes and soybeans are the source of protein while corn oil is added for the source of fat. C/STZ-induced rats were provided

ad libitum of standard diet coated with 6% cholesterol (Sigma-Aldrich®) for six weeks to induce hypercholesterolemia. C/STZ-induced rats were then injected with 45 mg/kg STZ (Sigma-Aldrich®) in fresh 0.1 M citrate buffer, pH 4.0 to induce hyperglycemic stage. The rats with fasting blood glucose of ≥ 200 mg/dL were considered as diabetic stage. Sericin and reverse osmosis water were fed by oral gavage to C/STZ-induced rats with and without sericin, respectively, for seven days.

Specimen collection

Blood collection and clinical chemistry. All rats were fasted for 6 h and humanly euthanized with an overdose of isoflurane® inhalation. Whole blood was collected from the heart and centrifuged at 1500 rpm for 10 min. Serum was then kept at –20°C. Blood clinical chemistry testing was conducted by accredited outsource laboratory. Blood glucose, lipid profiles, renal, and hepatic functions were performed by the Quality Control Division, National Laboratory Animal Center, Mahidol University. Serum lipase was measured by Bangkok Pathology Laboratory, Bangkok, Thailand.

Tissue collection. Liver, heart, kidney, and pancreas were collected, kept, and maintained on ice cold throughout all steps of each experiment. All of them were divided into three parts: (i) majority part for mitochondrial extraction; liver, heart, and kidney were immediately stored in ice-cold homogenized buffer as described in Fernandez-Vizarrá *et al.*¹⁷; for liver and kidney using buffer A (0.32 M sucrose, 1 mM EDTA, and 10 mM Tris-HCl, pH 7.4) and for heart using buffer AT (0.075 M sucrose, 0.225 M sorbitol, 1 mM EGTA, 0.1% fatty acid-free bovine serum albumin (BSA), and 10 mM Tris-HCl, pH 7.4); (ii) minority part for histopathological and immunohistochemical studies, all tissues were fixed with 10% neutral buffer formalin for 48 h; and (iii) resting part for electron microscopic studies, all tissues were primary fixed for 1 h with 2.5% glutaraldehyde in 0.1 M sucrose phosphate buffer (SPB), pH 7.4.

Mitochondrial extraction

Mitochondria were isolated as proposed by Fernandez-Vizarrá *et al.*¹⁷ with slight modifications. All livers, hearts, and kidneys from each group were pooled, weighed, cut into small pieces, and then consecutively washed for many times to remove blood and connective tissue. All cleaned tissues were subsequently homogenized in their own ice-cold homogenate buffer (A and AT) using a glass Elvehjem potter using a motor-driven Teflon pestle

Table 1 Amino acid composition of heat extraction sericin (in mole%)

Asp	Ser	Glu	Gly	His	Arg	Thr	Ala	Pro	Cys	Tyr	Val	Met	Lys	Ile	Leu	Phe
15.64	33.63	4.61	15.03	1.06	2.87	8.16	4.10	0.54	0.54	3.45	2.88	3.39	2.35	0.56	1.00	0.28

Ala: alanine; Arg: arginine; Asp: aspartic acid; Cys: cysteine; Glu: glutamic acid; Gly: glycine; His: histidine; Ile: isoleucine; Leu: leucine; Lys: lysine; Met: methionine; Phe: phenylalanine; Pro: proline; Ser: serine; Thr: threonine; Tyr: tyrosine; Val: valine.

with several up and down strokes at 600 rpm (for liver and kidney) and 900 rpm (for heart). The homogenates were twice centrifuged at 1000g, 4°C for 5 min to sediment unbroken tissue, cells, and nuclei. The supernatant was transferred to 1.5 mL Eppendorf tubes and centrifuged at 15,000g (for liver and kidney) or 9000g (for heart), 4°C for 2 min. The supernatant was removed with carefully eliminating all fat and fluffy layers on the top of pellet containing mitochondria. To eliminate harmful enzymes, nucleases, phospholipases, and proteases, the pellet from two Eppendorf tubes was combined, resuspended with 1.5 mL ice-cold buffers, and then centrifuged at 15,000g, 4°C for 2 min. The final pellet was resuspended in ice-cold final equilibrated buffer (250 mM sucrose, 5 mM KH₂PO₄, 10 mM Tris-HCl, 2 mg/mL BSA, pH 7.2). The mitochondrial extraction was separated in two parts: (i) for electron microscopic study, 200 µL of resuspended mitochondria was fixed in 2.5% glutaraldehyde in 0.1 M SPB for 1 h; (ii) for biochemical study, the remaining suspended mitochondria were kept at 4°C or on ice until testing was performed (no longer than 6–8 h). Mitochondrial protein content was measured by bicinchoninic acid assay.

Electron microscopic studies

All fixed tissues and isolated mitochondria were triplicate washed with 0.1 M SPB, 10 min each and secondary fixed with 1% osmium tetroxide in 0.1 M SPB for 1 h. After again washed with 0.1 M SPB, the specimens were dehydrated in graded ethanol, infiltrated with LR White resin (EMS®), embedded in capsule beams, and finally polymerized at 65°C for 48 h. All specimens were cut in 90–100 nm thickness and stained with uranyl acetate and lead citrate. The ultra-thin sections were investigated under transmission electron microscope (Hitachi; model HT7700, Japan). Ultrastructural changes in all tissues were evaluated by focusing on mitochondrial alterations and other related pathologies. From mitochondrial extraction, dysmorphic mitochondria, for instance vacuolation, swelling, and ghost form as mentioned in several reports,^{18,19} were examined, counted, and calculated to percentage/field at 3000X magnification.

Histopathological studies

All fixed specimens were dehydrated in graded ethanol, infiltrated and embedded in paraffin, sectioned to 4 µm thick, and stained with hematoxylin and eosin. All histopathological changes were examined under light microscope and scored the severity together with their distribution using four grades: 0: no lesion, 1: mild or <25%, 2: moderate or 25–60%, and 3: severe or >60%.

Immunohistochemical studies

To demonstrated oxidative and antioxidative properties of sericin, MDA and SOD were used as markers for immunohistochemical studies in liver, kidney, and pancreas. Polyclonal rabbit anti-MDA (Bioss, USA, GR233461) and polyclonal rabbit anti-Mn-SOD (Millipore, USA, 2683863) were used as primary antibodies. The sections were deparaffinized in xylene then rehydrated in ethanol, and

unmasked antigens in heated citrate buffer pH 6.0. The EnVision FLEX/HRP kit (DAKO, Denmark, K8002) was applied to block peroxidase activity and non-specific binding. The sections were incubated with primary antibody for 1 h and labeled polymer HRP anti-mouse/rabbit for 20 min and then visualized with diaminobenzidine chromogen. Finally, the sections were counterstained in hematoxylin and mounted with Permount®.

The expression of these two markers was assessed using the H-score, a multiplication of percentage area of expression (0–100) and intensity score (with four grades; 0 = negative staining, 1 = low intensity staining, 2 = moderate intensity staining, and 3 = strong intensity staining). The area of expression was measured by an imaging analysis program (ImageJ® Version 1.36; National Institutes of Health, Bethesda, Maryland, USA) as described in Ampawong and Aramwit.²⁰ Briefly, in each group, 10 color images of all tissues were randomly obtained using a light microscope (BX51, Olympus®) and digital camera (DP70, Olympus®) at 1000X magnification. Color images were converted to gray scale. The expression areas were then located by threshold adjustment and measured as percentage area of the expression/image.

Biochemical study

To prove the neutralized property of sericin on oxidative circumstance, liver mitochondrial extraction from C/STZ-induced rats without sericin was performed in this experiment. Extracted mitochondria were induced oxidative stress with 2.0 mM hydrogen peroxide (H₂O₂) (Merck, Germany) for 5 min at 25°C. Four doses of sericin, 10, 50, 75, and 100 µg/ml, were then added together with H₂O₂ for 30 min at 25°C to compare dose-response.

ROS is a well-known indicator for oxidative stress marker. The production of ROS was measured as described in Kobroob *et al.*²¹ The assay was based on fluorescent dye transformation from 2',7'-dichlorofluorescein diacetate (DCFDA) to DCF or non-fluorescent to highly fluorescent stages activating by ROS. Experimented mitochondria were incubated in 2 µM DCFDA at 25°C for 1 h. Highly fluorescent stage was measured at 485 nm excitation and 530 nm emission using a fluorescence microplate reader (VICTOR 3V Multi-label plate reader, PerkinElmer, USA). ROS level was calculated in terms of difference in optical density between excitation and emission stages.

Statistics

Statistical analysis was conducted using GraphPad Prism® version 5. The non-parametric *t*-test was used for group comparisons. The level of statistical significance was set at *p* < 0.05.

Results

Clinical signs and blood clinical chemistry

Obviously, growth rate and food intake, both C/STZ-induced rats with and without sericin, were gradually increased during the cholesterolemic induction periods (first to seventh week) and decreased during both

cholesterolemic and hyperglycemic induction periods (eighth week), as shown in Figure 1. In our experiment, high-cholesterol diet and STZ induced hypercholesterolemic and hyperglycemic conditions with severe diabetic signs such as polyuria, polydipsia, inappetite, weight loss, depression, ruffle fur, and emaciation in all rats, seven days post-induction. Blood clinical chemistry is presented in Table 2. Although blood cholesterol was significantly reduced after seven days of sericin fed, blood glucose still had significantly higher level in C/STZ-induced rats with and without sericin than sham rats. However, blood triglyceride, creatinine, alanine aminotransferase, lipase, and blood urea nitrogen had similar level in all groups that reflected normal liver and kidney function.

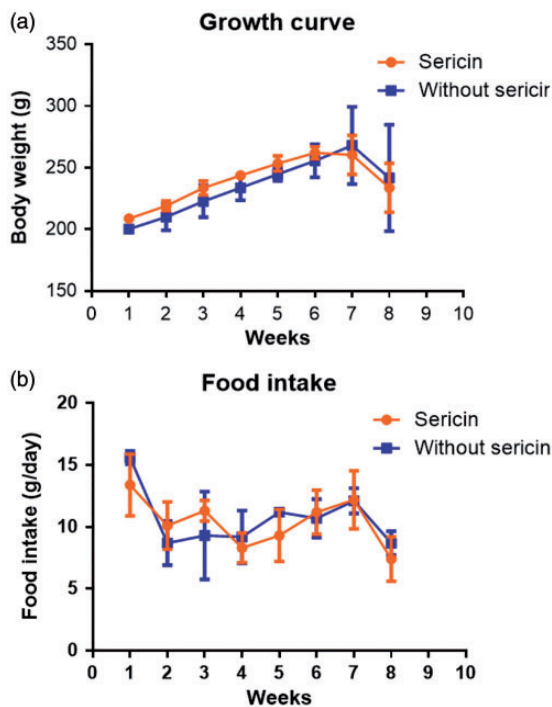


Figure 1 Growth rate (a) and food intake (b) in C/STZ-induced rats with and without sericin among all periods of the study. STZ: streptozotocin. (A color version of this figure is available in the online journal.)

Ultrastructural studies

Mitochondrial extraction. In order to determine fine morphology of mitochondria from heart, liver, and kidney extraction, electron microscopic study was performed. In general, intact mitochondria from the heart had more well-organized and packed cristae arrangement than seen in the liver and kidney exhibiting radiator or vesiculate appearance (Figure 2(a) to (r)). The results revealed that high blood cholesterol and glucose levels caused dysmorphic mitochondria range from mild to severe alteration characterized by (i) degenerative changes, e.g. matrix vacuolation, disarrangement of cristae, swelling, and partial cristolysis; (ii) necrosis characterized by complete cristolysis or ghost cells (Figure 2(a) to (r)). The prevalence of normal mitochondria from liver and heart in C/STZ-induced rats with sericin was significantly higher than those rats without sericin (Figure 2, S1 and T1). Conversely, swelling and ghost mitochondria from liver and heart in C/STZ-induced rats treated with sericin were significantly lower than those rats without sericin (Figure 2, S2 and T2). However, in kidney, the proportion of intact and dysmorphic mitochondria had similar in both groups (Figure 2, U1–2).

Ultrastructural changes (heart, liver, kidney, and pancreas). In this part, there were no quantitative results from mitochondria ultrastructural changes in the tissues since the prevalence of dysmorphic mitochondria had already been done in the mitochondrial extraction. Fine morphological changes were emphasized to compare the structure of mitochondria from all extractions and tissues with other related pathologies. In C/STZ-induced rats with and without sericin, high blood cholesterol and glucose caused myocardial and mitochondrial degeneration characterized by defibrillation or disarrangement of myofibril, discontinuous of Z-line, and intermyocardial mitochondria swelling (Figure 3(d) to (f)). Similar to heart mitochondria, liver mitochondria in the degenerative hepatocyte had swollen (Figure 3(j) to (l)) in both C/STZ-induced rats with and without sericin. However, it is surprising that mitochondria in the microvesicular steatotic hepatocyte remained intact (Figure 3(g) to (i)). In the kidney, the

Table 2 Blood clinical chemistry among normal rats and cholesterol/STZ-induced rats with and without sericin treatment.

Group	Serum chemistry						
	Cholesterol (mg/dL)	Triglyceride (mg/dL)	Glucose (mg/dL)	BUN (mg/dL)	Creatinine (mg/dL)	ALT (U/L)	Lipase (U/L)
Normal (sham's)	110.66 ± 4.76 ^a	88.00 ± 10.39	154.50 ± 6.06 ^{a,b}	17.06 ± 0.67	0.20 ± 0.00	44.00 ± 2.30	27.00 ± 9.00
Sericin-cholesterol/STZ	151.00 ± 10.74 ^b	133.33 ± 23.37	240.50 ± 71.31 ^a	20.05 ± 3.60	0.32 ± 0.02	69.25 ± 2.95	34.33 ± 3.84
w/o Sericin-cholesterol/STZ	232.50 ± 15.56 ^{a,b}	125.75 ± 12.87	226.0 ± 27.54 ^b	19.26 ± 3.04	0.22 ± 0.03	68.40 ± 12.10	34.00 ± 4.04
Kruskal-Wallis p value	0.012	0.161	0.001	0.816	0.06	0.188	0.760

STZ: streptozotocin.

^{a,b}Match significance difference at $p < 0.05$ with Dunn's multiple comparisons test.

Bold values indicate significant differences ($p < 0.05$)

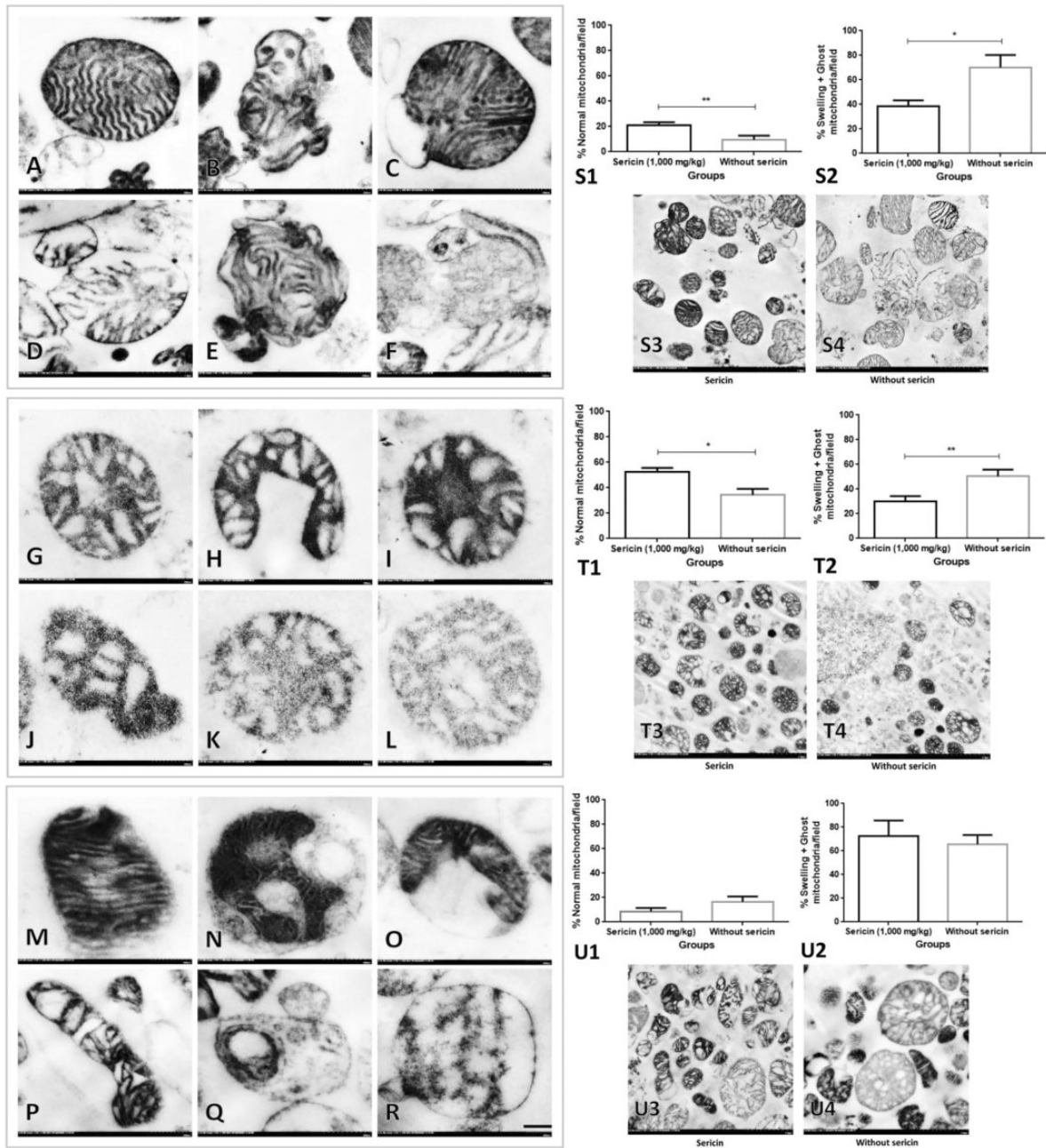


Figure 2 Dysmorphic mitochondria from heart, liver, and kidney extraction in high-cholesterol diet/STZ rat with and without sericin. Intact heart mitochondria (a) with normal cristae and complete membrane boundary when compared to swelling mitochondria (b–e) characterized by the presence of matrix distension and cristae disarrangement with partial cristolysis and ghost mitochondria (f) characterized by complete cristolysis, electron-lucent matrix, and incomplete membrane boundary. Mitochondrial alteration from the liver exhibited the vesiculate appearance with different degree of matrix distension referred to as cellular swelling (g–j) and ghost mitochondria (k–l) were similarly seen in the heart. Intact mitochondria from kidney (m) represented the electron-dense matrix and packed cristae without vacuolation and vesiculate appearance that had seen in swelling mitochondria (n–p). Ghost mitochondria from kidney are indicated in (q) and (r). Bar graphs and electron micrographs comparing the prevalence of normal and dysmorphic mitochondria in the heart, liver, and kidney are shown in S1–4, T1–4, and U1–4, respectively. **p* value < 0.05; ***p* value < 0.01. STZ: streptozotocin

number of mitochondria was located in proximal and distal tubules (Figure 3(m)). Hypercholesterolemic and hyperglycemic conditions in C/STZ-induced rats with and without sericin-induced tubular degeneration exhibited loss of epithelial mitochondria, swelling mitochondria, degenerative nuclei, and endoplasmic reticulum alteration (Figure 3(o) to (r)). The results obviously suggest that mitochondrial

structures in all examined tissues are similar to those from the extractions. Degenerative cells usually presented dysmorphic forms. Interestingly, the results demonstrated that unlike C/STZ-induced rats treated with sericin and sham rats, giant degenerative mitochondria and peculiar dense-dark endoplasmic reticulum (ER) were found in C/STZ-induced rats without sericin and deposited

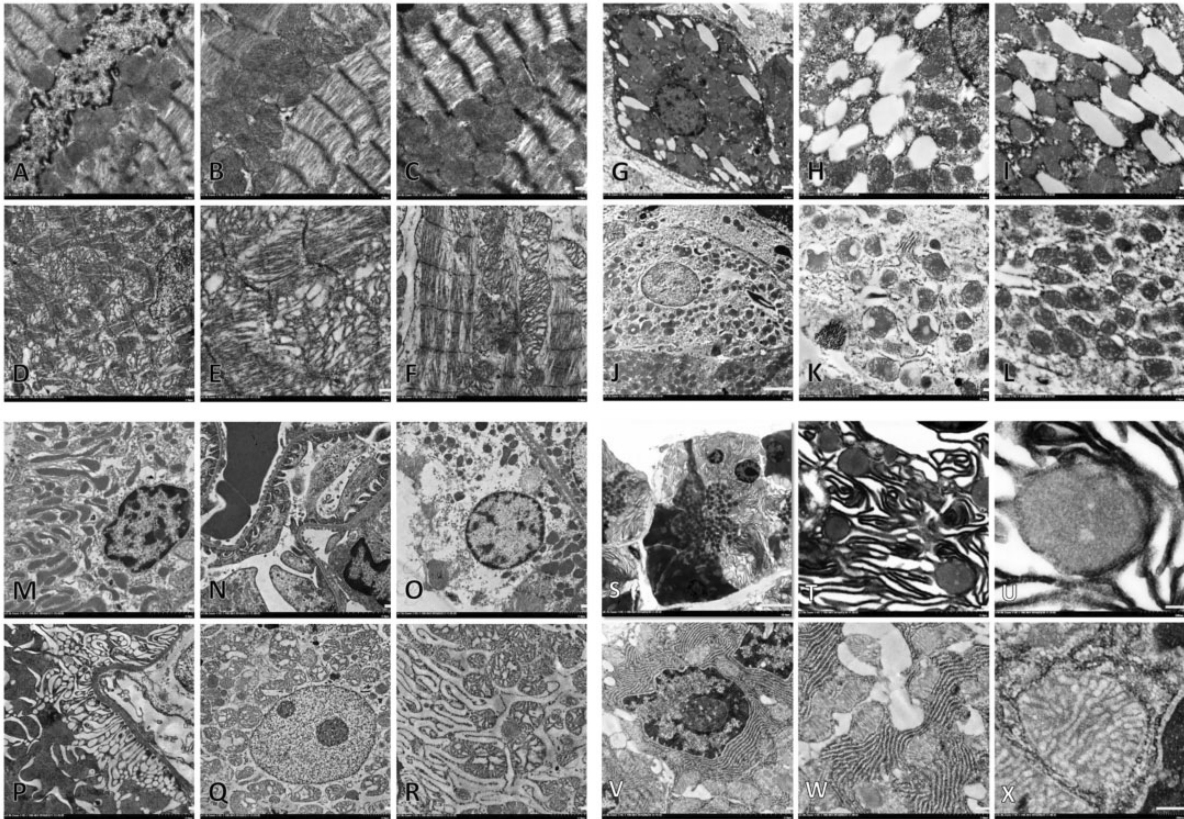


Figure 3 Ultrastructural changes in the heart, liver, kidney, and pancreas. Intact cardiac myofibril and intermyocardial mitochondria (a–c) compared to degenerative myofibril with disorganization of Z-line and mitochondrial swelling (d–f). Hepatocyte with microvesicular steatosis indicated by cytoplasmic fat droplet accumulation beside to a number of intact mitochondria (g–i) compared to degenerative hepatocyte with swollen and sparse mitochondria (j–l). Intact proximal tubule with packed mitochondria (m) and glomerular capillary bed characterized by complete filtration slit and mesangial matrix (n) compared to degenerate epithelium with mitochondrial loss (o and p), swollen mitochondria (q and r), alternative endoplasmic reticulum (ER) (r). Degenerative pancreatic acinar gland exhibited disarrangement of peculiar dense and dark ER with interspace distension and degenerative enlargement mitochondria (s–u) compared to the intact gland composed of well-organized ER and intact mitochondria (v–x)

throughout of the degenerate pancreatic exocrine gland (Figure 3(s) to (u)).

Histopathology

High cholesterolemic stage led to fat deposit in the cytoplasmic hepatocyte called microvesicular steatosis. C/STZ-induced rats without sericin had significantly higher score of steatosis when compared to those rats treated with sericin (Figure 4(a) to (c)). However, hyperglycemic effect caused degenerative Islet of Langerhans in both C/STZ-induced rats with and without sericin. Cellular hypertrophy, pyknosis, and vacuolation were observed (Figure 5(a) to (d)). Interestingly, degenerative exocrine gland in pancreas was only found in C/STZ-induced rats without sericin. The pathological changes were included with the significant depletion of zymogen granules and cytoplasmic disorganization (Figure 6(a) to (c)) in association with ER alteration from electron microscopic studies (Figure 3(s) to (u)). In kidney, the diabetic rats with or without sericin treatment had similar histopathological findings particularly mild to moderate tubular degeneration with sparse inflammation; however, the glomeruli, pelvis, and the other areas were intact.

Oxidative stress markers

To demonstrate antioxidative property of sericin on affected tissues in hypercholesterolemia and hyperglycemia rats, MDA and SOD were used as oxidative and antioxidative markers, respectively. In liver (Figure 4(d) to (f)) and exocrine gland pancreas (Figure 6(d) to (f)), C/STZ-induced rats without sericin had significantly higher MDA expression than the rats treated with sericin. In kidney (Figure 7) and Islet of Langerhans (Figure 5(e) to (g)), there was no difference of MDA expressions between rats treated with and without sericin. The positive immunolabeling was located on several areas as shown in Figure 4(d) and (e). Interestingly, MDA was higher expressed on glomerulus and proximal tubule than collecting duct in cholesterolemic and diabetic rats in contrast to normal rats (Figure 7).

Mitochondrial ROS production

To confirm antioxidative property of sericin, ROS production was measured in liver-extracted mitochondria. The results revealed that all doses of sericin-treated mitochondria had lower level of ROS production when compared to H_2O_2 -induced oxidative stress and non-treatment

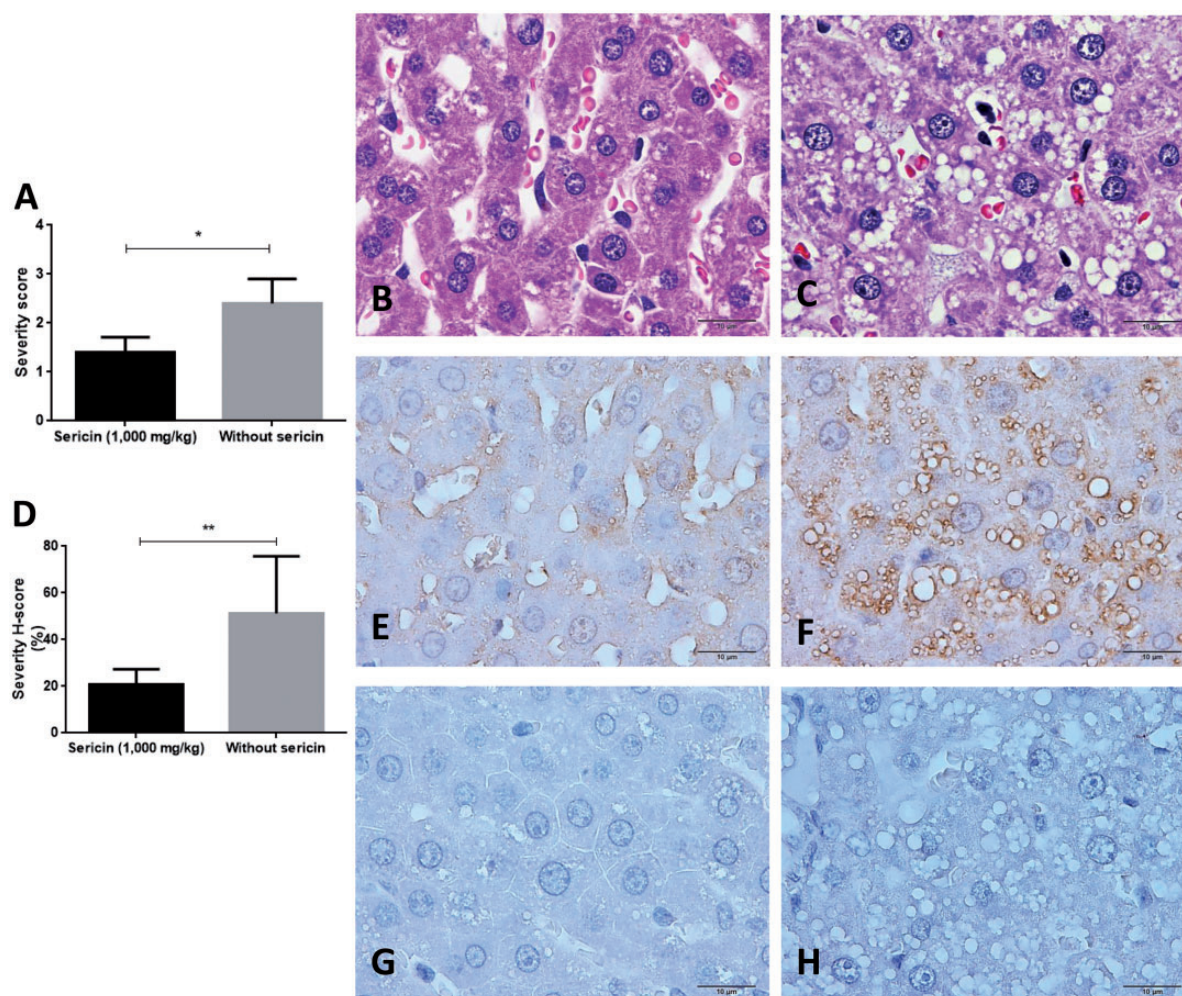


Figure 4 Severity score of hepatic steatosis, MDA, and SOD immunolabeling in the liver. Bar graph compared the severity score of steatosis between C/STZ-induced rats with and without sericin (a), histological changes in C/STZ-induced rats with (b) and without sericin (c) indicated by micro-fat droplet depositing in cytoplasmic hepatocyte (H&E staining). Bar graph of the MDA expression score between C/STZ-induced rats with and without sericin (d), a number of positive immunoreactive areas were located on hepatic sinusoid and fat vacuole, MDA predominately expressed in C/STZ-induced rats without sericin (f) compared to C/STZ-induced rats with sericin (e). Contrast to SOD marker which has no expression in both groups of C/STZ-induced rats with (g) and without (h) sericin. **p* value < 0.05; ***p* value < 0.01. H&E: hematoxylin and eosin; MDA: malondialdehyde; SOD: super-oxide dismutase; STZ: streptozotocin. (A color version of this figure is available in the online journal.)

mitochondria (Figure 8). However, dose-responses were not observed.

Discussion

Sericin has long been encouraged to use for many aspects in biomedical field, for example, wound dressing material as reported in our previous studies.^{20,22-26} The other points of view, sericin has also been a candidate for development of functional food or adjunctive therapeutic agent against other non-communicable diseases such as hypercholesterolemia and diabetes mellitus (DM).^{13,14,27-29} Several mechanisms not only antioxidative property of sericin,¹² but its catabolic effect to fat metabolism is also discussed.^{13,14,27} However, no one has studied on the impact of sericin to improve mitochondrial function and integrity since their alteration involves many diseases particularly in high cholesterol and DM. The present study is the first report that suggests sericin improves heart and liver mitochondrial integrity in high blood cholesterol and glucose

conditions due to (i) its antioxidative property as shown by the reduction of liver mitochondrial ROS production and down-regulation of hepatocyte MDA expression and (ii) its inhibitory effect of fat anabolism to reduce the severity of microvesicular steatosis that corresponds to the previous studies.^{13,27} The close correlation between mitochondrial function and steatosis formation has been postulated. Although mitochondria are considered as cholesterol-poor organelles, excess cholesterol load may cause cholesterol deposition to their membrane or matrix and play a crucial step in disease progression, e.g. steatohepatitis, carcinogenesis, and Alzheimer disease.³⁰

With regard to ultrastructural changes in the mitochondria, morphological alterations were correlated with cell death.³¹ Our study highlighted that mitochondrial alteration is caused by an oxidative stress consequence to DM and hypercholesterolemia. From the extraction, dysmorphic mitochondrial structure ranged from degenerative to necrotic stages characterized by swollen to ghost

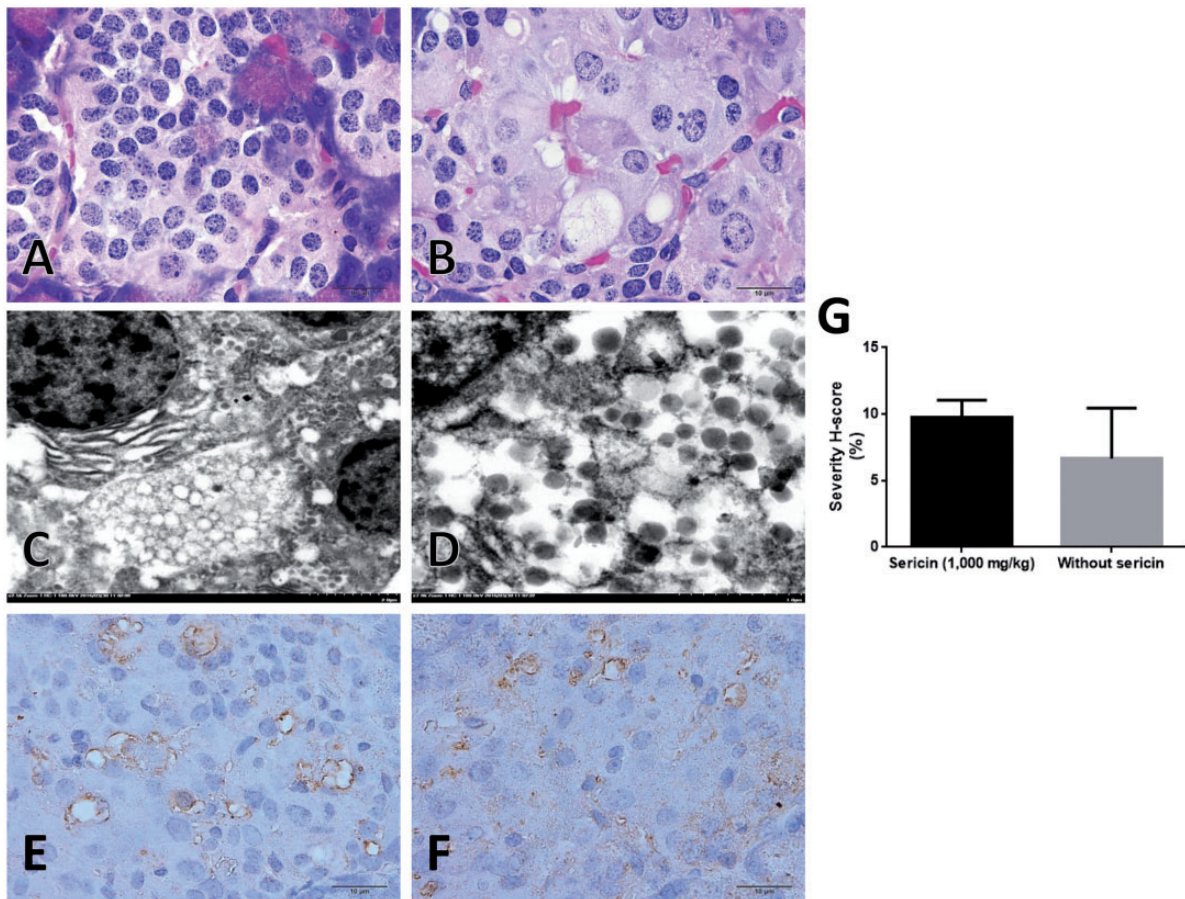


Figure 5 Islet of Langerhans morphology and its MDA immunolabeling. Intact Islet of Langerhans (a) compared to the degenerative one from C/STZ-induced rats that showed cellular hypertrophy, vacuolated cell, and pyknotic nuclei (b) (H&E staining). Ultrastructure of delta cell demonstrated many typical electron-lucent granules with vacuolated cell degeneration (c and d). Positive immunoreaction was located on vacuolated cells and small blood vessels both in C/STZ-induced rats with (e) and without sericin (f), bar graph of the MDA expression score between C/STZ-induced rats with and without sericin (g). H&E: hematoxylin and eosin; MDA: malondialdehyde; STZ: streptozotocin. (A color version of this figure is available in the online journal.)

formation, respectively. Likewise, mitochondria from the degenerative cells, e.g. hepatocyte, tubular epithelium, or exocrine pancreatic gland were also obviously changed as seen in the extraction. Vesiculated, vacuolated, swelled, and ghost mitochondrial are the terms used to describe the severity of dysmorphic mitochondria characterized by the connection of inner membrane to lamellar cristae with crista junction to form multiple vesicular matrix compartments. Interestingly, vesiculated mitochondria appear in association with the release of cytochrome C during the initiative phase of apoptosis.³²

Apart from antioxidative ability and preventive effect of lipid accumulation of sericin, we attempted to figure out other roles of its hypocholesterolemic property. Since the results exhibited that sericin preserves endoplasmic reticulum and zymogen granule in exocrine gland pancreas which synthesizes and stores several digestive enzymes principally prolipase. Recently, there is possibility that tissue lipoprotein lipase (e.g. heart, liver, and muscle) or lipase supplement can lower triglyceride and cholesterol levels.³³ It is found that normocholesterolemic men have high lipase activity.³⁴ Taken together, up-regulation of lipase mRNA expression enhances lipolysis.³⁵ Unfortunately, our

study presents that sericin has no effect to increase serum lipase within a short period of ingestion. In order to get better understanding of this effect, longer period of sericin ingestion needs to be conducted. Moreover, the role of sericin on the level of tissue lipase activity and integrity of pancreatic gland relates to hypocholesterolemia that needs to be further studied. In addition, it is well described that cholesterol absorption is composed of several processes facilitated by the formation of lipid complex form; "micelles," cholesterol absorption inhibitors on enterocyte provide a potential role to prevent and treat hypercholesterolemia.³⁶ Recently, *in vitro* studies claimed that lowering cholesterol effect of sericin is described through the inhibitory effect of cholesterol absorption from intestinal cell and micelles formation.¹⁴ However, *in vivo* studies still need to be further proven.

Considering amino acid composition of sericin, it is very difficult to predict that which amino acid conspicuously plays an important role in cholesterol reduction and mitochondrial improvement. Collectively, the highest amino acid component in sericin is serine that is required for fat metabolism.³⁷ Endogenous serine is a source for phosphatidylserine (PS) synthase enzymes that catalyze the

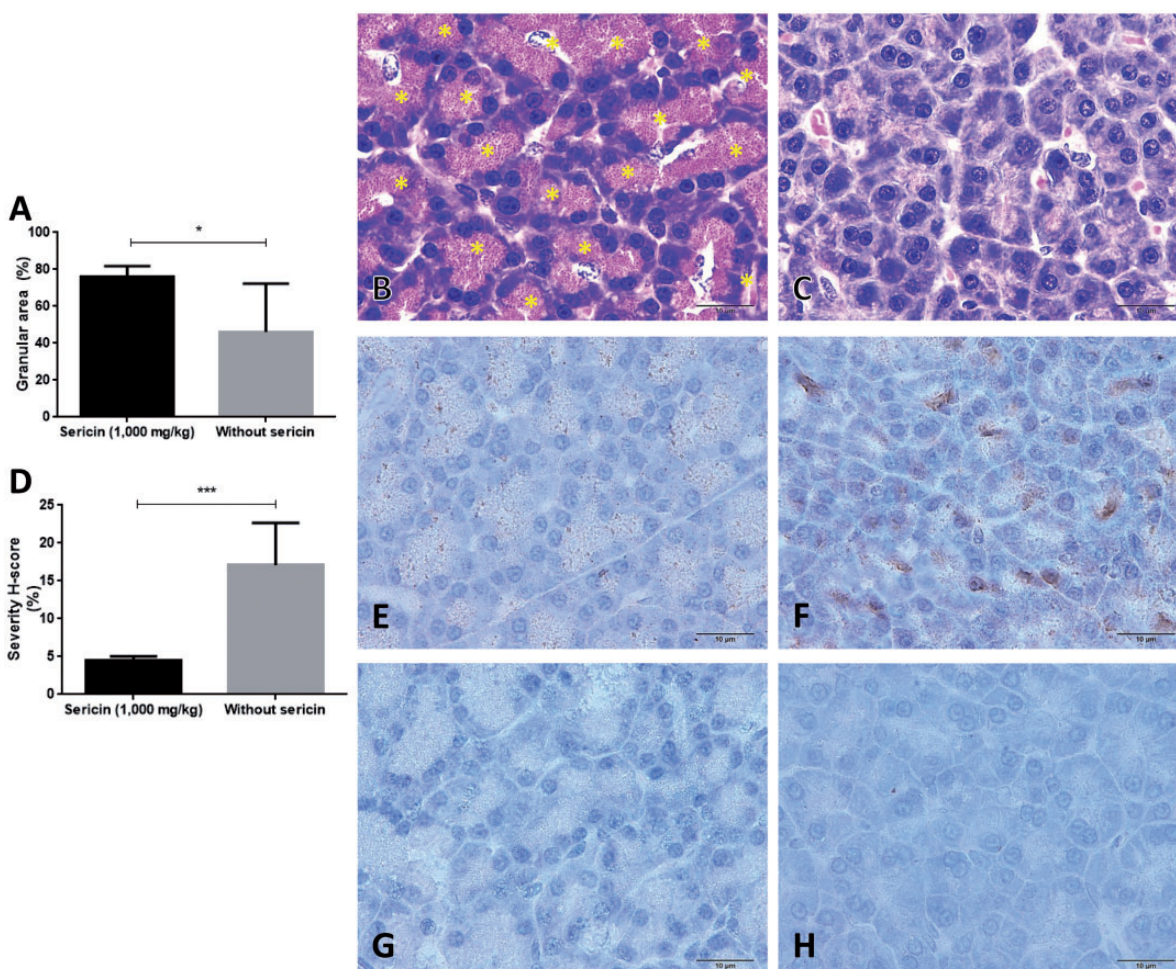


Figure 6 Exocrine pancreatic gland morphology and its MDA and SOD immunolabeling. Bar graph exhibited the zymogen granule density in exocrine gland (a), histomorphology of acinar gland pancreas; a number of zymogen granules were stored inside the cells of C/STZ-induced rats with sericin (b) contrast to C/STZ-induced rats without sericin (c). Bar graph of the MDA expression score between C/STZ-induced rats with and without sericin (d), a number of positive immunoreactive areas were located on glandular cells and zymogen granules storage area in C/STZ-induced rats without sericin (f) compared to C/STZ-induced rats with sericin (e). Contrast to SOD marker which has no expression in both groups of C/STZ-induced rats with (g) and without sericin (h). **p* value < 0.05. MDA: malondialdehyde; SOD: superoxide dismutase; STZ: streptozotocin. (A color version of this figure is available in the online journal.)

production of PS, a crucial element for protection of cell from excess lipids.³⁸ Down-regulation of PS synthases and PS is affiliated with non-alcoholic steatohepatitis.³⁹ In addition, it is known that other than PS, L-serine also participates in alcoholic fatty liver amelioration.⁴⁰ Taken together, mitochondrial ROS production is regulated by serine through redox reaction to support mitochondrial survival and growth.⁴¹ Therefore, it can be hypothesized that serine, a greatest amino acid in sericin, may be a key component to modulate hypocholesterolemia, hepatic steatosis, and mitochondrial alteration in C/STZ-induced rats. On the other hand, different extraction method of sericin results in dissimilar amino acid content. Particularly heat extraction gives high content of methionine as presented in our previous study in contrast to the other extraction by urea, base, and acid. Consequently, some studies postulate that low methionine content in their sericin may be involved in the lowering effect of blood cholesterol on account of some intestinal absorptive effects of low methionine or incorporation with low-apoprotein secretion from liver.¹⁴

In our study, sericin failed to reduce blood glucose as seen by it has not enough effect to preserve mitochondrial integrity in the kidney and the up-regulation of oxidative stress marker (MDA) in Islet of Langerhans cells, glomeruli, and proximal tubules. The latter evidence may be related to the deviate function of those tissues characterized by insulin production and glucose absorption in Langerhans cell and proximal tubule, respectively. Moreover, in this study, low dose of STZ with hypercholesterolemia gave severe disease outcome leading to incapability to reduce blood glucose with sericin ingestion. The mechanistic details of the hypoglycemic effect of sericin need to be further studied. In general, DM mitochondrial structure in affected tissues is smaller in size, loss of cristae, increase electron-dense granules, lipid droplet deposition, and swollen,⁴² as presented in our results.

In summary, sericin modulates blood cholesterol, hepatic fat deposition, dysmorphic mitochondria, and ER alterations in C/STZ-induced rats through its antioxidative property. These findings may express that sericin composes

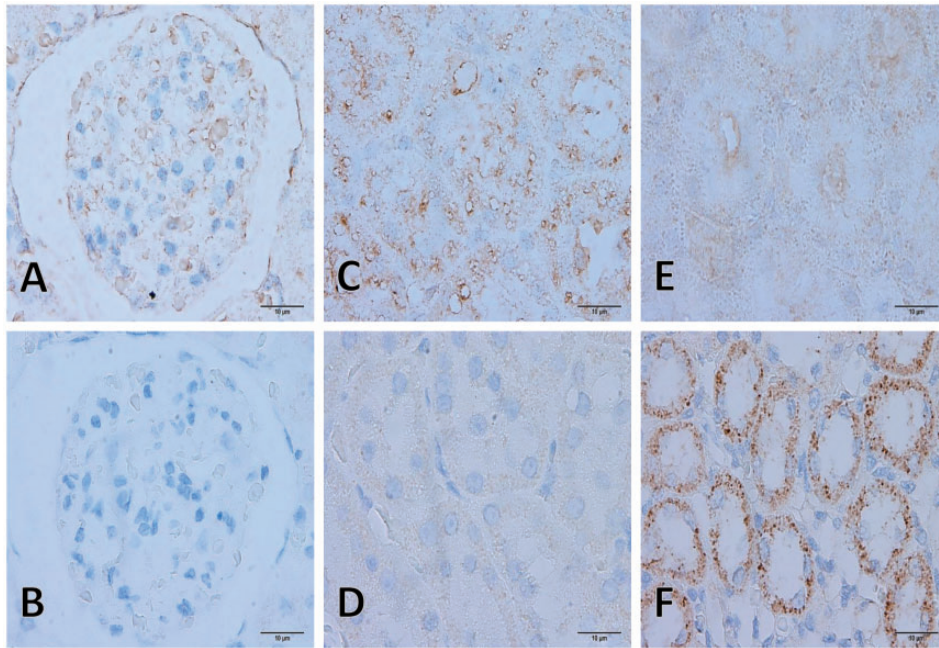


Figure 7 MDA and SOD immunolabeling on kidney. MDA expression was only found in C/STZ-induced rats with and without sericin (a, c, and e) contrast to SOD which was only found in sham's rats (b, d, and f). Glomerular MDA expression (a), the positive reaction was located on capillary, erythrocyte, and parietal layer of Bowman's capsule. Tubular MDA expression was intense localized on cytoplasmic tubular epithelium in the proximal tubule (c) while very faint in collecting duct (e). Tubular SOD expression was strongly labeled on cytoplasmic tubular epithelium in the collecting duct (f) while negative immunoreaction on glomerulus and proximal tubule (b and d). MDA: malondialdehyde; SOD: super-oxide dismutase; STZ: streptozotocin. (A color version of this figure is available in the online journal.)

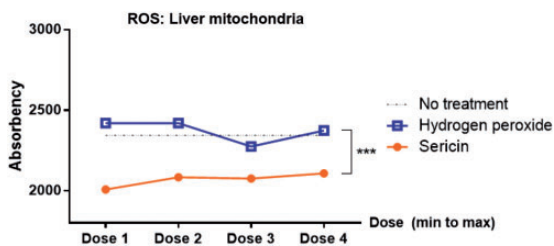


Figure 8 Mitochondrial ROS production. Line graph indicated the mitochondrial ROS production in the extraction from liver. (A color version of this figure is available in the online journal.)

of beneficial effects for further utilization as an additive in functional food.

Authors' contributions: All authors participated in the design, interpretation, and analysis of the studies; SA and DI conducted the experiments, PA supplied critical reagents (e.g. sericin, high-cholesterol diet, and other chemicals), planned the experiments, and analyzed the data. All authors wrote, revised, and approved the final manuscript.

ACKNOWLEDGEMENTS

This research has been supported by Grant for International Research Integration: Chula Research Scholar from The Ratchadaphiseksomphot Endowment Fund, Chulalongkorn University (Grant Number GCURP_59_17_33_02).

DECLARATION OF CONFLICTING INTERESTS

The author(s) declared no potential conflicts of interest with respect to the research, authorship, and/or publication of this article.

REFERENCES

- Wilson DF, Harrison DK, Vinogradov SA. Oxygen, pH, and mitochondrial oxidative phosphorylation. *J Appl Physiol* 2012;**113**:1838–45
- Wang L, Liu X, Nie J, Zhang J, Kimball SR, Zhang H, Zhang WJ, Jefferson LS, Cheng Z, Ji Q, Shi Y. ALCAT1 controls mitochondrial etiology of fatty liver diseases, linking defective mitophagy to hepatosteatosis. *Hepatology* 2014;**61**:486–96
- Zou X, Yan C, Shi Y, Cao K, Xu J, Wang X, Chen C, Luo C, Li Y, Gao J, Pang W, Zhao J, Zhao F, Li H, Zheng A, Sun W, Long J, Szeto IM, Zhao Y, Dong Z, Zhang P, Wang J, Lu W, Zhang Y, Liu J, Feng Z. Mitochondrial dysfunction in obesity-associated nonalcoholic fatty liver disease: The protective effects of pomegranate with its active component punicalagin. *Antioxid Redox Signal* 2014;**21**:1557–70
- Fiorentino TV, Prioleta A, Zuo P, Folli F. Hyperglycemia-induced oxidative stress and its role in diabetes mellitus related cardiovascular diseases. *Curr Pharm Des* 2013;**19**:5695–703
- Khoshjou F, Dadras F. Mitochondrion and its role in diabetic nephropathy. *Iran J Kidney Dis* 2014;**8**:355–8
- McCommis KS, McGee AM, Laughlin MH, Bowles DK, Baines CP. Hypercholesterolemia increases mitochondrial oxidative stress and enhances the MPT response in the porcine myocardium: beneficial effects of chronic exercise. *Am J Physiol Regul Integr Comp Physiol* 2011;**301**:R1250–8
- Le Lay S, Simard G, Martinez MC, Andriantsitohaina R. Oxidative stress and metabolic pathologies: from an adipocentric point of view. *Oxid Med Cell Longev* 2014;**2014**:908539

8. Guo C, Sun L, Chen X, Zhang D. Oxidative stress, mitochondrial damage and neurodegenerative diseases. *Neural Regen Res* 2013;**8**:2003-14
9. Gonzalez-Alonso A, Ramirez-Tortosa CL, Varela-Lopez A, Roche E, Arribas MI, Ramirez-Tortosa MC, Giampieri F, Ochoa JJ, Quiles JL. Sunflower oil but not fish oil resembles positive effects of virgin olive oil on aged pancreas after life-long coenzyme q addition. *Int J Mol Sci* 2015;**16**:23425-45
10. Sun L, Jin Y, Dong L, Sui HJ, Sumi R, Jahan R, Hu D, Li Z. *Coccomyxa gloeobotrydiformis* improves learning and memory in intrinsic aging rats. *Int J Biol Sci* 2015;**11**:825-32
11. Yamamoto H, Morino K, Mengistu L, Ishibashi T, Kiriyama K, Ikami T, Maegawa H. Amla enhances mitochondrial spare respiratory capacity by increasing mitochondrial biogenesis and antioxidant systems in a murine skeletal muscle cell line. *Oxid Med Cell Longev* 2016;**2016**:1735841
12. Li YG, Ji DF, Chen S, Hu GY. Protective effects of sericin protein on alcohol-mediated liver damage in mice. *Alcohol Alcohol* 2008;**43**:246-53
13. Okazaki Y, Kakehi S, Xu Y, Tsujimoto K, Sasaki M, Ogawa H, Kato N. Consumption of sericin reduces serum lipids, ameliorates glucose tolerance and elevates serum adiponectin in rats fed a high-fat diet. *Biosci Biotechnol Biochem* 2010;**74**:1534-8
14. Limpeanchob N, Trisat K, Duangjai A, Tiyaboonchai W, Pongcharoen S, Sutherawattananonda M. Sericin reduces serum cholesterol in rats and cholesterol uptake into Caco-2 cells. *J Agric Food Chem* 2010;**58**:12519-22
15. Aramwit P, Damrongsakkul S, Kanokpanont S, Srichana T. Properties and antityrosinase activity of sericin from various extraction methods. *Biotechnol Appl Biochem* 2010;**55**:91-8
16. Aramwit P, Kanokpanont S, Nakpheng T, Srichana T. The effect of sericin from various extraction methods on cell viability and collagen production. *Int J Mol Sci* 2010;**11**:2200-11
17. Fernandez-Vizarrá E, Ferrin G, Perez-Martos A, Fernandez-Silva P, Zeviani M, Enriquez JA. Isolation of mitochondria for biogenetical studies: an update. *Mitochondrion* 2010;**10**:253-62
18. Mariappan N, Soorappan RN, Haque M, Sriramula S, Francis J. TNF- α -induced mitochondrial oxidative stress and cardiac dysfunction: restoration by superoxide dismutase mimetic Tempol. *Am J Physiol Heart Circ Physiol* 2007;**293**:H2726-37
19. Zou LY, Zheng BY, Fang XF, Li D, Huang YH, Chen ZX, Zhou LY, Wang XZ. HBx co-localizes with COXIII in HL-7702 cells to upregulate mitochondrial function and ROS generation. *Oncol Rep* 2015;**33**:2461-7
20. Ampawong S, Aramwit P. Tolerogenic responses of CD206+, CD83+, FOXP3+, and CTLA-4 to sericin/polyvinyl alcohol/glycerin scaffolds relevant to IL-33 and HSP60 activity. *Histol Histopathol* 2016;**31**:1011-27
21. Kobroob A, Chattipakorn N, Wongmekiat O. Caffeic acid phenethyl ester ameliorates cadmium-induced kidney mitochondrial injury. *Chem Biol Interact* 2012;**200**:21-7
22. Aramwit P, Palapinyo S, Srichana T, Chottanapund S, Muangman P. Silk sericin ameliorates wound healing and its clinical efficacy in burn wounds. *Arch Dermatol Res* 2013;**305**:585-94
23. Aramwit P, Sangcakul A. The effects of sericin cream on wound healing in rats. *Biosci Biotechnol Biochem* 2007;**71**:2473-7
24. Aramwit P, Siritienthong T, Srichana T, Ratanavaraporn J. Accelerated healing of full-thickness wounds by genipin-crosslinked silk sericin/PVA scaffolds. *Cells Tissues Organs* 2013;**197**:224-38
25. Siritienthong T, Ratanavaraporn J, Aramwit P. Development of ethyl alcohol-precipitated silk sericin/polyvinyl alcohol scaffolds for accelerated healing of full-thickness wounds. *Int J Pharm* 2012;**439**:175-86
26. Siritientong T, Angspatt A, Ratanavaraporn J, Aramwit P. Clinical potential of a silk sericin-releasing bioactive wound dressing for the treatment of split-thickness skin graft donor sites. *Pharm Res* 2014;**31**:104-16
27. Okazaki Y, Tomotake H, Tsujimoto K, Sasaki M, Kato N. Consumption of a resistant protein, sericin, elevates fecal immunoglobulin A, mucins, and cecal organic acids in rats fed a high-fat diet. *J Nutr* 2011;**141**:1975-81
28. Seo CW, Um IC, Rico CW, Kang MY. Antihyperlipidemic and body fat-lowering effects of silk proteins with different fibroin/sericin compositions in mice fed with high fat diet. *J Agric Food Chem* 2011;**59**:4192-7
29. Song Z, Zhang M, Xue R, Cao G, Gong C. Reducing blood glucose levels in T1DM mice with an orally administered extract of sericin from hIGF-I-transgenic silkworm cocoons. *Food Chem Toxicol* 2014;**67**:249-54
30. Garcia-Ruiz C, Mari M, Colell A, Morales A, Caballero F, Montero J, Terrones O, Basanez G, Fernandez-Checa JC. Mitochondrial cholesterol in health and disease. *Histol Histopathol* 2009;**24**:117-32
31. Perkins G, Bossy-Wetzell E, Ellisman MH. New insights into mitochondrial structure during cell death. *Exp Neurol* 2009;**218**:183-92
32. Sun MG, Williams J, Munoz-Pinedo C, Perkins GA, Brown JM, Ellisman MH, Green DR, Frey TG. Correlated three-dimensional light and electron microscopy reveals transformation of mitochondria during apoptosis. *Nat Cell Biol* 2007;**9**:1057-65
33. Larsson M, Caraballo R, Ericsson M, Lookene A, Enquist PA, Elofsson M, Nilsson SK, Olivecrona G. Identification of a small molecule that stabilizes lipoprotein lipase in vitro and lowers triglycerides in vivo. *Biochem Biophys Res Commun* 2014;**450**:1063-9
34. Grandjean PW, Crouse SF, Rohack JJ. Influence of cholesterol status on blood lipid and lipoprotein enzyme responses to aerobic exercise. *J Appl Physiol* 2000;**89**:472-80
35. Lee J, Jun W. Methanolic extract of turmeric (*Curcuma longa* L.) enhanced the lipolysis by up-regulation of lipase mRNA expression in differentiated 3T3-L1 adipocytes. *Food Sci Biotechnol* 2009;**18**:1500-4
36. Wang DQ. Regulation of intestinal cholesterol absorption. *Annu Rev Physiol* 2007;**69**:221-48
37. Maddocks OD, Berkers CR, Mason SM, Zheng L, Blyth K, Gottlieb E, Vousden KH. Serine starvation induces stress and p53-dependent metabolic remodelling in cancer cells. *Nature* 2013;**493**:542-6
38. Mardinoglu A, Agren R, Kampf C, Asplund A, Uhlen M, Nielsen J. Genome-scale metabolic modelling of hepatocytes reveals serine deficiency in patients with non-alcoholic fatty liver disease. *Nat Commun* 2014;**5**:3083
39. Gorden DL, Ivanova PT, Myers DS, McIntyre JO, VanSaun MN, Wright JK, Matrisian LM, Brown HA. Increased diacylglycerols characterize hepatic lipid changes in progression of human nonalcoholic fatty liver disease; comparison to a murine model. *PLoS One* 2011;**6**:e22775
40. Sim WC, Yin HQ, Choi HS, Choi YJ, Kwak HC, Kim SK, Lee BH. L-serine supplementation attenuates alcoholic fatty liver by enhancing homocysteine metabolism in mice and rats. *J Nutr* 2015;**145**:260-7
41. Ye J, Fan J, Venneti S, Wan YW, Pawel BR, Zhang J, Finley LW, Lu C, Lindsten T, Cross JR, Qing G, Liu Z, Simon MC, Rabinowitz JD, Thompson CB. Serine catabolism regulates mitochondrial redox control during hypoxia. *Cancer Discov* 2014;**4**:1406-17
42. Sivitz WI, Yorek MA. Mitochondrial dysfunction in diabetes: from molecular mechanisms to functional significance and therapeutic opportunities. *Antioxid Redox Signal* 2010;**12**:537-77

(Received September 3, 2016, Accepted October 19, 2016)